STING-dependent induction of neutrophilic asthma exacerbation in response to house dust mite

Yasmine Messaoud-Nacer, Elodie Culerier, Stéphanie Rose, Isabelle Maillet, Boussad Rania, Chloé Veront, Florence Savigny, Bernard Malissen, Urszula Radzikowska, Milena Sokolowska, et al.

STING-dependent induction of neutrophilic asthma exacerbation in response to house dust mite.

Yasmine Messaoud-Nacer, PhD[1], Elodie Culerier, MSc[1], Stéphanie Rose, MSc[1], Isabelle Maillet, MSc[1], Bernard Malissen, PhD[2], Urszula Radzikowska, PhD[3,4], Milena Sokolowska, MD[3,4], Gabriel VL da Silva, PhD[5], Michael R Edwards, PhD[6], David J Jackson, PhD[6], Sebastian L Johnston, MD, PhD[6], Bernhard Ryffel, MD, PhD[1], Valerie F. Quesniaux, PhD[1], and Dieudonnée Togbe, PhD[1*]

ORCID ID : DT (0000-0001-6658-414X); VFQ (0000-0003-2907-7995), BR (0000-0003-2897-8230), SLJ (0000-0003-3009-9200); MS (0000-0001-9710-6685), UR (0000-0002-7341-9764), BM (0000-0003-1340-9342).

[1]*Experimental and Molecular Immunology and Neurogenetics, INEM UMR7355 University of Orleans and CNRS, 3B Rue de la Ferollerie 45100 Orleans-Cedex 2, France.*

[2]*Centre d'Immunophénomique (CIPHE), Aix Marseille Université, INSERM, CNRS, 13288, Marseille, France.*

[3]*Swiss Institute of Allergy and Asthma Research (SIAF), University of Zurich, Herman-Burchard-Strasse 9, 7265 Davos Wolfgang, Switzerland*

[4]*Christine Kühne – Center for Allergy Research and Education (CK-CARE), Herman-Burchard-Strasse 1, 7265 Davos Wolfgang,*

[5]*Ribeirão Preto Medical School, University of Sao Paulo. Avenida Bandeirantes, 3900 - CEP 14049-900. Ribeirao Preto, Sao Paulo, Brazil.*

[6]*National Heart and Lung Institute, Imperial College Londont, London W2 1PG, United Kingdom; Asthma UK Centre in Allergic Mechanism of Asthma, London, United Kingdom; Imperial College Healthcare NHS Trust, The Bays, S Wharf Rd, London W2 1NY, United Kingdom.*

**Corresponding author: Dieudonnée Togbe (dtogbe@cnrs-orleans.fr)*

Running head: STING activation induces neutrophilic asthma exacerbation

Acknowledgements

The authors thank Glen N. Barber for sharing the STING-deficient mice, to Zhijian J. Chen for providing cGAS-deficient mice (University of Texas Southwestern Medical Center, Dallas), to Nicolas Manel for sharing STING-OST^{fl} mice (Institut Curie, PSL Research University, INSERM U932, Paris, France). The skillful assistance of David Gosset, running the MO2VING platform (CNRS UPR 4301, Orleans) and Marie-Laure Dessain (TAAM, CNRS UAR44) are gratefully acknowledged.

Abstract (248 words)

Background: Severe refractory, neutrophilic asthma remains an unsolved clinical problem. STING agonists induce a neutrophilic response in the airways, suggesting that STING activation may contribute to the triggering of neutrophilic exacerbations. We aim to determine whether STING-induced neutrophilic lung inflammation mimics severe asthma.

Methods: We developed new models of neutrophilic lung inflammation induced by house dust mite (HDM) plus STING agonists diamidobenzimidazole (diABZI) or cGAMP in wild-type, and conditional-STING-deficient mice. We measured DNA damage, cell death, NETs, cGAS/STING pathway activation by immunoblots, N1/N2 balance by flow cytometry, lung function by plethysmography, and Th1/Th2 cytokines by multiplex. We evaluated diABZI effects on human airway epithelial cells from healthy or patients with asthma, and validated the results by transcriptomic analyses of rhinovirus infected healthy controls *vs* patients with asthma.

Results:

DiABZI administration during HDM challenge increased airway hyperresponsiveness, neutrophil recruitment with prominent $NOS2^{+}ARG1^{-}$ type 1 neutrophils, protein extravasation, cell death by PANoptosis, NETs formation, extracellular dsDNA release, DNA sensors activation, IFNγ, IL-6 and CXCL10 release. Functionally, STING agonists exacerbated airway hyperresponsiveness. DiABZI caused DNA and epithelial barrier damage, STING pathway activation in human airway epithelial cells exposed to HDM, in line with DNA-sensing and PANoptosis pathways upregulation and tight-junction downregulation induced by rhinovirus challenge in patients with asthma.

Conclusions: Our study identifies that triggering STING in the context of asthma induces cell death by PANoptosis, fueling the flame of inflammation through a mixed Th1/Th2 immune

response recapitulating the features of severe asthma with a prognostic signature of type 1 neutrophils.

Keys words: DNA sensing, cGAMP, diABZI, cell death, asthma exacerbation.

Abbreviations

AHR: airway hyperresponsiveness, AIM2: absent in melanoma 2, BAL, BronchoAlveolar Lavage; BALF, BronchoAlveolar Lavage Fluid; cGAMP: cyclic Guanosine monophosphate-Adenosine MonoPhosphate, cGAS: cyclic GMP-AMP synthase, DDX41: DEAD-box helicase 41, diABZI: symmetry-related amidobenzimidazole-based compounds, GSDMD: Gasdermin D, GEO: Gene Expression Omnibus, hAEC, human airway epithelial cells, HBEC: human bronchial epithelial cells, HDM: house dust mite, HE: hematoxylin and eosin, IFI204: IFN-γ-Inducible protein 204, IRF3: IFN regulatory factor 3, ISG: Interferon Stimulated Gene, LDH: Lactate DeHydrogenase, MLKL: Mixed Lineage Kinase domain Likepseudokinase, MPO: myeloperoxidase, NETs: Neutrophil Extracellular Traps, NLRP3: NOD-, LRR- and Pyrin Domain-Containing Protein 3, PAS: Periodic acid Schiff, RNA-Seq : RNA sequencing, STING: STimulator of INterferon Genes, TBK1: TANK-binding kinase 1, WT: wild type, ZBP1: Z-DNA-Binding Protein 1.

Introduction (455 words)

The most common reaction to several allergens such as house-dust mite (HDM) in allergic asthma endotype is IgE production depending on high Th2 responses with IL-4, IL-5 and IL-13 release, mucus overproduction, eosinophil recruitment, epithelial metaplasia and airway remodeling [1]. The ability of an allergen to initiate the first steps of type 2 immune response is based on direct epithelial cell damage and damage of associated cells forming the respiratory barrier. Allergenic toxins or proteases may cause necrotic cell death leading to a strong Th2 response [2]. Severe asthma is often associated with Th2 low and mixed endotype, increased neutrophils and extracellular DNA (eDNA) in patient sputum, with an increase in type 1 cytokines IL-1β and IL-6 at the late onset of the disease, and unresponsiveness to corticosteroids or specific biologicals [1,3-6]. However, the molecular mechanism underlying severe neutrophilic asthma is more complex and remains unsolved.

Extracellular host-derived DNA has been associated with allergic type 2 immune responses. Indeed, host DNA released from dying cells acts as a damage associated molecular pattern (DAMP) that mediates e.g. the adjuvant activity of alum [7]. The detection of extracellular host-derived dsDNA is ensured by cyclic GMP–AMP synthase (cGAS) which converts ATP and GTP into cyclic dinucleotide 2'3'cGAMP. The latter, in turn binds and activates the ER-resident adaptor protein Stimulator of Interferon Genes (STING) which activates the transcription factors NF-kB and IRF3, and the production of pro-inflammatory cytokines including tumor necrosis factor (TNFα), IL-6 and type I IFNs (IFNα/β) [8].

Cytosolic dsDNA accumulated in airway epithelia of ovalbumin (OVA)- or HDM-challenged mice [9]. Deletion of cGAS in airway epithelial cells attenuated OVA or HDM induced allergic airway inflammation, while cGAS promoted Th2 immunity likely by regulating airway epithelial GM-CSF [9]. Further, 2'3'cGAMP or c-di-GMP produced after activation of cGAS by extracellular DNA, was shown to function as an adjuvant promoting type 2 allergic lung

inflammation when administered during sensitization with HDM, with increased of serum IgE and eosinophils in the airways, an effect mediated by IL-33 and STING signaling pathway [10,11].

Recently, we showed that endotracheal administration of cGAMP or the synthetic STING agonist diamidobenzimidazole (diABZI) led to lung inflammation with neutrophilic response in the broncho-alveolar space, cell death via PANoptosis, loss of epithelial barrier function, and release of self-dsDNA and NETs [12].

Here, we asked whether activating STING pathway during challenges after immunization with the widely distributed house-dust mite allergen might affect the allergic response and trigger a neutrophilic exacerbation. We show that cGAMP and furthermore diABZI administration during challenge in mice exacerbated HDM-induced lung resistance, cell death by PANoptosis, neutrophil recruitment with a prominent N2 to N1 switch, protein extravasation and extracellular dsDNA release in the airways, with an overexpression of Th1 cytokine IFNγ. We report differential expression of DNA-sensing and PANoptosis pathways after rhinovirus challenge in patients with asthma.

Methods (565 words)

Mice

Female C57BL/6Rj mice were purchased from Janvier Laboratories (Le Genest St Isle, France). Wild type mice and mice deficient for STING (STING$^{-/-}$) [13] , cGAS (cGAS$^{-/-}$) [14] were bred and housed under specific pathogen free conditions at CNRS animal facility (TAAM UAR44, Orleans, France). STING-OST^{fl} were crossed to LysM^{Cre} mice to generate STING-OST^{fl} LysM^{cre} mice. They were maintained in a 12-h light-dark cycle with food and water ad libitum, following European and local legislation. Age-matched, 8- to 12- week-old mice were used for experiments. All animal experiments complied with the French Government animal experiment regulations and ARRIVE guidelines. The protocols were submitted to the "Ethics Committee for Animal Experimentation of CNRS Campus Orleans" under the number CLE CCO 2019-2017 and 2020-2006, and approved by the French Minister under APAFIS #25876 and #26195.

Induction of allergic airway inflammation and bronchoalveolar lavage (BAL)

Mice were anesthetized with 2% Isoflurane (ISO-VET, Netherlands) were sensitized with HDM on day 0 and 7 (25 µg/mouse, i.n.) and challenged with HDM (Stallergenes Greer) intranasally on 3 consecutive days (10 µg/mouse, i.n. on day 14-16), in the absence or together with cGAMP (at 1, 3 or 10 µg/mouse, i.t.), diABZI compound 3 (at 0.1 or 1 µg/mouse, i.t) or Poly(I:C) (at 60 or 200 µg/mouse, i.t). Mice were analyzed on day 17, 24 hours after the last HDM instillation (Fig. 1A).

Bronchoalveolar lavage (BAL) was performed 24h after the last challenge by flushing lung tissue four times with 0.5 mL of cold NaCl 0.9% via tracheal intubation with a cannula. BALF was collected, cells counted and cytospins performed. The supernatant of the first lavage was collected after centrifugation and stored at -80°C for dsDNA and mediator quantifications. The left lung lobe was harvested for histology, the post caval lung for RNA extraction and qPCR analysis and the right lobes for Western blot analysis and cytokine measurement. Protein

extravasation in the BALF was measured by Pierce™ BCA Protein Assay (ThermoFisher®, Massachusetts).

Cell Culture and stimulation

Human airway epithelial cells (hAEC; Epithelix, Switzerland) isolated from bronchial biopsies (passage 1) were maintained in 75 cm^2 flasks in the hAEC serum-free culture medium (Epithelix). hAEC (passage 8) were seeded in 24-wells plate at 5 x 10^5 cells/well, when they reached 80% confluence. Cells were stimulated with HDM at 100 µg/mL alone or in combination with diABZI (10 µM), cGAMP (14 µM) or Poly(I:C) (100 µg/mL) for 2 or 24h at 37°C and 5% CO2. Human airway bronchial epithelium (MUCILAIR™; Epithelix, Switzerland), from a single healthy or donor with asthma were maintained in MUCILAIR™ serum-free medium (Epithelix) and stimulated on the apical face, with HDM at 100 µg/mL alone or in combination with diABZI, cGAMP or Poly(I:C) as above for 6h. Supernatant from hAEC and MUCILAIR™ cultures were collected for mediator measurements and cells harvested for mRNA and proteins analysis.

Statistical Analysis

Statistical analysis was performed with GraphPad Prism 9.0 software (San Diego). To determine whether the data come from Gaussian distribution, column statistic using Shapiro-Wilk normality test is performed before running the statistical analysis. Statistical significance was determined by non-parametric Kruskal-Wallis multiple-comparisons tests followed by Dunn post-test or two-way ANOVA followed by Dunn post-test as indicated in figure legends. All data are shown as mean ± SEM. Saline control data are compared with HDM group. HDM -/+ agonist groups are compared. P value <0.05 was considered significant. *p <0.05, **p <0.01, ***p <0.001 and ****p <0.0001.

Results (2614 words)

Synthetic STING agonist diABZI triggers a neutrophilic asthma exacerbation in HDM sensitized mice.

To evaluate how STING activation by agonists modulate type 2 immune response, we tested their effects during the challenge phase of HDM-induced allergic lung inflammation in mice. We compared the effect of the natural STING agonist cGAMP, and of the potent, non-nucleotidyl STING agonist diABZI [15], to the TLR3 agonist dsRNA Poly(I:C), all known to induce IRF3-type 1 IFN response. Wild type BL6 (WT) mice sensitized with HDM on day 0 and 7 (25 µg/mouse, i.n.) and challenged on day 14-16 (10 µg/ mouse, i.n.) received either diABZI (1 µg/mouse, i.t.), cGAMP (10 µg/mouse, i.t.), or Poly(I:C) (200 µg/mouse, i.t.), doses determined from previous titrations (**Suppl Fig E1-3**), and were analyzed on day 17, 24-hours after the last challenge (**Fig 1A**). First, we evaluated airway hyperresponsiveness (AHR), one of the hallmarks of allergic asthma known to correlate with disease severity [16,17]. There was a significant increase of AHR in HDM-challenged WT mice at a dose of 200 mg/mL of methacholine (MCh), as compared to saline control (**Fig 1B**). Administration of diABZI during HDM challenge further increased AHR significantly, while cGAMP increased AHR only at 200 mg/mL of MCh, and Poly(I:C) had no effect, compared to untreated HDM-challenged mice (**Fig 1B**). DiABZI and cGAMP administration had little effect on eosinophil recruitment in the airways (**Fig 1C**), while they strongly increased neutrophil recruitment (**Fig 1D)** in HDM-challenged mice. Interestingly, diABZI and cGAMP promoted a subsets of neutrophils expressing inducible nitric oxide synthase (iNOS/NOS2) corresponding to type 1 neutrophils (N1, $NOS2^{+}ARG1^{-}$) while decreased the frequency of arginase 1 (ARG1) expressing type 2 neutrophils (N2, $NOS2^{-}ARG1^{+}$) (**Fig 1E**, **Suppl Fig E4A-D**). This increase in N1 neutrophils

was associated with higher myeloperoxidase (MPO) in BALF and lung (**Fig 1F-G**), total protein extravasation (**Suppl Fig E4E**) and dsDNA release in BALF (**Fig 1H**). There was also an increase in macrophages, but not in lymphocytes influx in BAL (**Suppl Fig E4A-C**) or Th2 cytokines IL-4, IL-5 and IL-13 (**Suppl Fig E4F-K**). The exacerbation effect was observed especially with diABZI, inducing a strong IFNγ response (**Fig 1I**) with CCL11, IL-6 and TNF release in the airways (**Suppl Fig E4L-P**). Further, IFNα/β, the end-products of STING pathway activation were increased in BALF upon diABZI administration (**Fig 1J, K**).

STING agonists induced a narrowing of the airways with severe infiltration of inflammatory cells in the peribronchial area, epithelial injury, bronchiolitis, alveolitis and decreased goblet cells hyperplasia and production of mucus together with a decrease in *Muc5ac* transcripts in the lung compared to HDM-challenged mice (**Fig 1L-P**), while TLR3 agonist caused no major changes (**Fig 1L-O**). Muc5AC protein concentration doubled in BALF after administration of STING or TLR3 agonists while it was essentially unaffected in the lung (**Fig 1Q-R**). STAT6, the transcription factor involved in *Muc5ac* gene induction and mucus hypersecretion [18] was phosphorylated in the lung of HDM challenged mice and this was increased by STING or TLR3 agonists (**Fig 1S, Suppl Fig E4Q**).

Thus, administration of the potent STING agonist diABZI during HDM challenge augmented HDM-induced lung resistance, together with a strong neutrophilic response characterized by neutrophil recruitment, MPO expression, protein extravasation, overexpression of Th1 cytokine IFNγ and extracellular dsDNA release in the airways.

NETosis and PANoptosis as main sources of airway dsDNA fueling STING-triggered exacerbation of HDM inflammation.

Extracellular dsDNA release is an active process in several chronic inflammatory diseases. Therefore, we first assessed the ability of neutrophils to form NETs [19,20]. Indeed, MPO staining demonstrated that unlike HDM-treated mice that showed localized cellular staining, the lung of cGAMP- and more importantly diABZI-challenged mice exhibited the typical morphological shape of NETs (**Fig 2A**), with citrullinated histone H3 (Cit-H3) revealed by immunoblot (**Fig 2B, suppl Fig E5A**). In contrast, Poly(I:C) did not result in the formation of NET, with intracellular MPO staining and absence of Cit-H3 (**Fig 2A-B**). DNA damage was documented by increased pγH2AX after both diABZI and cGAMP challenges, but less after Poly(I:C) administration (**Fig 2B, suppl Fig E5A**).

NETs comprise host DNA fibers coated with cytoplasmic proteases, making host DNA available to activate DNA sensors. Indeed, cGAS, IFI204 and/or DDX41 expression increased in the lung of HDM and STING agonist challenged mice (**Fig 2C, suppl Fig E5B**). Further, there was evidence of inflammasome activation, likely involving AIM2 and/or NLRP3, with non-canonical caspase-11 upregulation, resulting in cleavage of IL-1β and IL-18 release after STING trigger (**Fig 2D, suppl Fig E5C**).

NETs associated molecules such as MPO, neutrophil elastase and defensins may promote lung injury, and directly induce epithelial and endothelial cell death [19,21]. HDM-immunized and challenged mice co-administered with STING or TLR3 agonists induced caspase 3 cleavage indicative of apoptosis in the lung tissue, but also cell death markers of necroptosis and pyroptosis with upregulation of Mixed Lineage Kinase domain Likepseudokinase (MLKL) and Gasdermin D (GSDMD), and GSDMD cleavage indicative of PANoptosis (**Fig 2E, suppl Fig E5D**). We further assessed specific components of the macromolecular complexes regulating PANoptosis by immunoblot. Indeed, Z-DNA binding protein 1 (ZBP1), caspase-8 and RIPK3 were upregulated after challenge with STING or TLR3 agonists in HDM-treated mice (**Fig 2E, suppl Fig E5D**). We also demonstrated a co-localization of PANoptosis components Caspase-

8, ASC and RIPK3 proteins in macrophages from BAL cells (**Fig 2F**) which is absent in neutrophils (**Suppl Fig E5E**).

Therefore, neutrophils induced during HDM challenge with STING agonists undergo NETs formation, expose host DNA to activate innate immune DNA sensors, inducing lung tissue damage and death by PANoptosis, amplifying DNA release as a positive feedback loop.

STING dependence of the neutrophilic exacerbation of HDM-induced response.

To evaluate the STING specificity of diABZI induced asthma exacerbation, response to the extracellularly released dsDNA, mice deficient for STING ($STING^{-/-}$) or cGAS ($cGAS^{-/-}$) were sensitized and challenged with HDM with or without diABZI as above (**Fig 3A**). DiABZI-induced increase of neutrophils was absent in the airways of HDM-challenged $STING^{-/-}$ mice, and reduced in $cGAS^{-/-}$ mice (**Fig 3B**), as were total inflammatory cells, macrophages and lymphocytes, or the decreased recruitment of eosinophils (**Suppl Fig E6A-D**). In addition, diABZI-induced increase of MPO and extracellular dsDNA (**Fig 3C-E**), or protein extravasation, IFNγ, TNF, IL-6, and CXCL10 (**Fig 3F-K**) release were abolished in the airways of HDM-challenged $STING^{-/-}$ mice, while they were barely affected in $cGAS^{-/-}$ mice. Because allergic airway inflammation triggers Th2 immune response, we evaluated Th2 cytokines and found increased IL-4 and IL-5 transcripts and proteins in HDM-challenged mice (**Suppl Fig E6E, F** and **H, I**). DiABZI further increased Th2 cytokine IL-13 and chemokines CCL11 and CCL24 in the airways, and this was absent in $STING^{-/-}$ and reduced in $cGAS^{-/-}$ mice (**Suppl Fig E6 G, J-L**). Pulmonary $CXCR2^{+}$ and $CXCR4^{+}$ expressing neutrophils subsets increased after diABZI challenge were reduced in $STING^{-/-}$ and $cGAS^{-/-}$ mice (**Suppl Fig E6 O-R**).

The increased leukocyte infiltration, epithelial injury, with decreased goblet cells, mucus staining (**Fig 3L-O**) and *Muc5ac* transcript expression (**Fig 3P**) after diABZI administration in HDM-challenged WT mice were abolished in $STING^{-/-}$ mice, while they were barely affected

in cGAS$^{-/-}$ mice. DiABZI and HDM co-administration upregulated *Tmem173* (STING) transcript expression in WT and cGAS$^{-/-}$ mice (**Fig 3Q**), while the increase in *Mb21d1* (cGAS) transcripts was abolished in STING$^{-/-}$ mice (**Fig 3R**).

IL-13 mRNA expression, a Th2 cytokine necessary for mucus metaplasia, increased after diABZI and HDM co-administration in WT mice, while it was barely affected in STING$^{-/-}$ or cGAS$^{-/-}$ mice. IL-13 binding triggers a STAT6-dependent transcriptional program involving the activation of Serpin1 and Clca1 (protein calcium-activated chloride channel 1) whose transcripts were overexpressed after diABZI administration in HDM-challenged WT mice but not in STING$^{-/-}$ mice (**Fig 3S-V**). On the other hand, the transcripts for *Socs1*, a negative regulator of *Muc5ac* expression [22], was overexpressed after diABZI co-administration in WT mice but not in STING$^{-/-}$ mice (**Fig 3W**), in line with the fact that STING activation was shown to enhance SOCS1 expression [23].

Thus, diABZI-induced asthma exacerbation is mediated by STING pathway activation in terms of neutrophil recruitment, release of extracellular dsDNA and pro-inflammatory cytokines in the airways, increased epithelial injury with decreased goblet cells and mucus production, while the involvement of cGAS is more limited.

STING-deficient macrophages and granulocytes mitigate asthma exacerbation in vivo.

Neutrophilic inflammation is observed during asthma exacerbation but also in the airways of patients with severe asthma [24]. In addition to neutrophils, macrophages are one of the main lung cell types responsible for the uptake of cGAMP *in vivo* [25]. We investigated the contribution of both cell types in mice by generating conditional STING deficient mice. We crossed mice carrying STING-OST floxed alleles (STING-OST^{fl}) with LysM^{cre} transgenic mice expressing Cre under the control of the LysM promotor to obtain STING-OST^{fl}LysM$^{cre/+}$ mice deficient for STING gene in myeloid cells such as granulocytes and macrophages, as well as STING-

297 OST^{fl}LysM$^{+/+}$ control mice (**Suppl Fig E7 A-D**). Administration of cGAMP during HDM
298 challenges resulted in a reduction of eosinophils and an increase in total cells, neutrophils, MPO
299 and self dsDNA in BALF of STING-OST^{fl}LysM$^{+/+}$ control mice (**Fig4 A-E** and **Suppl Fig**
300 **E7E, G**). These parameters were partially reduced in STING-OST^{fl}LysM$^{cre/+}$ suggesting that
301 myeloid cells, but also other cell types contribute to shape the neutrophilic response after
302 STING trigger (**Fig4 A-E**). cGAMP induced an increase in type I IFNα/β, as well as pro-
303 inflammatory cytokines TNFα and IL-6 production in HDM-treated STING-OST^{fl}LysM$^{+/+}$
304 control mice that were partially reduced in STING-OST^{fl}LysM$^{cre/+}$ (**Fig 4 F-I**). The increase in
305 peribronchial leukocytes infiltration and epithelial injury following cGAMP administration in
306 STING-OST^{fl}LysM$^{+/+}$ mice was abrogated in STING-OST^{fl}LysM$^{cre/+}$ (**Fig 4J, K**). Moreover,
307 protein extravasation in BALF was reduced in STING-OST^{fl}LysM$^{cre/+}$ mice in comparison with
308 control mice (**Suppl Fig E7F**), which was suggestive of a less severe barrier disruption.
309 Neutrophils infiltrating the lung of mice lacking STING in granulocytes/macrophages, were
310 tested for their ability to form NETs. BAL cells from STING-OST^{fl}LysM$^{+/+}$ control mice
311 challenged with HDM and cGAMP showed the formation of a weblike structure positive for
312 MPO and Cit-H3 staining (**Fig 4L**), suggestive of NET formation. In contrast, this process was
313 reduced in STING-OST^{fl}LysM$^{cre/+}$ group (**Fig 4L**), in line with the reduced histopathological
314 damage observed.
315 Thus, these data indicate that granulocytes/macrophages, but also other cell types, contribute to
316 the development of STING-dependent neutrophilic asthma exacerbation *in vivo*.
317
318 **Epithelial cells respond to diABZI and may contribute to STING agonist-induced**
319 **neutrophilic asthma exacerbation.**
320 Allergens cause airway epithelium damage and structural changes including downregulation of
321 group I tight junction and extracellular matrix (ECM) expression which are often associated
322 with asthma exacerbations and severity [26-28]. The transmembrane proteins Zona-occludens-1

(ZO-1) are scaffold proteins important for cell-cell adhesion in healthy tissue and main regulators of epithelial permeability in allergic lung inflammation [27]. After confirming the role of diABZI on immune cells infiltration, we investigated its effect on human airway epithelium. HDM led to ZO-1 downregulation in lung tissue compared to saline control (**Fig 5A**), as expected [27]. STING agonists DiABZI and cGAMP, and Poly(I:C) further downregulated ZO-1 expression as evidenced by immunofluorescence staining (**Fig 5A**). To evaluate the ability of diABZI to activate STING pathway in epithelial cells, human airway epithelial cells (hAEC) from bronchial biopsies were stimulated for 2h or 24h with HDM alone or in combination with diABZI, cGAMP or Poly(I:C). There was evidence of STING pathway activation with the detection of phosphorylated STING, TBK1 and IRF3 when hAEC were co-stimulated with diABZI detectable at an early stage, 2h post stimulation (**Fig 5B, suppl Fig E8A**). cGAMP and Poly(I:C) co-stimulation also induced TBK1 phosphorylation at 2h, that persisted after 24h with diABZI and cGAMP. Moreover, there was evidence of epithelial DNA damage in hAEC, revealed by phosphorylation of γH2AX at 2h and 24h post stimulation (**Fig 5C, suppl Fig E8A**), and some activation of necroptosis with the phosphorylation of MLKL at 2h (**Fig 5C, suppl Fig E8A**). Activating STING with diABZI in cells sensitized with HDM yielded in the secretion of inflammatory cytokines starting from 2h post stimulation that were sustained after 24h, such as CXCL8, IFNβ, CXCL10, IL-6 and TNF-α (**Fig 5 D-M**).

To further characterize the contribution of epithelial barrier, air liquid interface (ALI) culture of bronchial epithelial cells isolated from the lung of healthy donor and patient with asthma were performed and stimulated for 16h with HDM alone or in combination with diABZI, cGAMP or Poly(I:C (**Fig 5 N**). DiABZI induced an increased release of lactate dehydrogenase (LDH), IFNα, IFNβ, IFNλ, CXCL10, IL-6 and TNF-α protein and overexpression of *MUC5AC* transcript in healthy epithelial cells sensitized with HDM (**Fig 5 O-V**), and less in epithelial cells from patient with asthma (**Fig 5 O-V**). Further, diABZI induced epithelial DNA damage

evidenced by the phosphorylation of γH2AX in epithelial cells from patient with asthma, compared to healthy cells (**Fig 5 W**).

Thus, diABZI affected airway epithelium cells by activating STING pathway, impairing tight junctions, and inducing epithelial DNA damage, necroptosis and secretion of inflammatory cytokines, that may further fuel the lung inflammation.

Viral infection of human bronchial epithelial cells from patients with asthma aggravates inflammation and weakens epithelial barrier both *in vitro* and *in vivo*.

To ascertain the clinical relevance of these findings, we first analyzed the different expression of STING and PANoptosis pathways in PBMC from healthy controls or patients with severe asthma **(Suppl FigE9)**. Indeed, host double-stranded DNA released by NETosis promote rhinovirus-induced asthma exacerbations [29]. Therefore, we analyzed DNA-sensing, PANoptosis, tight junction, and neutrophils gene signatures from two independent studies addressing Rhinovirus (RV) infection in patients with asthma, either *in vitro* in differentiated primary bronchial epithelial cells (HBECs) from healthy and individuals with asthma [30], or *in vivo* in bronchial brushing from intranasally RV infected healthy controls and patients with asthma [31,32] (**Supl FigE10**).

Human epithelial cells from patients with asthma stimulated *in vitro* with RV-A16 **(Fig. 6A)** showed an upregulation of genes involved in DNA-sensing and STING pathway **(Fig.6B)** such as the DNA sensors ZBP1, IFI16 and the cytosolic TRIM21. *IRF3* responsible of type I/III IFNs induction and anti-viral defense was also upregulated in the cells of these patients, concomitant with *IFN-λ* expression, while STING itself was not significantly downregulated. Analysis of tight-junction gene sets **(Fig.6C)** revealed the reduced expression of a whole cluster of genes such as *OCLN, CLD3, CLDN4, NRAS, HCLS1, MYH10* in virus-infected cells from patients with asthma in comparison to the controls. Moreover, analysis of PANoptosis related genes set

revealed the upregulation and a tendency to upregulation of several components of the PANoptosome such as the pivotal *ZBP1*, *PYCARD*, *CASPASE-8*, *RIPK1*, *CASPASE-1*, and *FADD* after viral infection of the cells from patients with asthma compared to the controls **(Fig.6D)**, which was not visible before RV infection **(Suppl Fig E10A-D)**. Mucus genes such as *MUC5AC* and *MUC5B* were also upregulated **(Suppl Fig E10E-F)**.

Bronchial brushings from patients with asthma experimentally infected *in vivo* with RV-A16[31] **(Fig. 6E)** showed a decrease in a group of tight junction-related gene such as *CLDN15, TJAP1, AKT2, SRC, CGN, EXOC3, LLG2, CLDN22,* compared to similarly infected healthy controls, while *CLDN12* and *MYL12B* genes were increased **(Fig. 6F)**. PANoptosis components showed a tendency toward an increase 4 days after *in vivo* infection in patients with asthma compared to controls **(Fig.6G)**, in contrast to the non-infected controls and patients with asthma, where the PANoptosis components were downregulated **(Suppl Fig E9G-I)**. Moreover, the gene expression of IL-18 (*IL18*) was higher after infection in patients with asthma compared to healthy individuals **(Fig.6G)**, in line with inflammasome activation[32]. Interestingly, the NOS2/ARG1 gene expression balance was disrupted in bronchial brushings. *NOS2* was significantly increased after infection in patients with asthma compared to the controls, while *ARG1* was downregulated in patients with asthma **(Fig.6H-I).** Overall, these analyses show an involvement of DNA sensing pathway, weakening of the epithelial barrier and upregulation of pro-inflammatory markers such as *NOS2* after RV infection in patients with asthma.

Discussion (791 words)

Here we demonstrate the existence of a tight link between STING activation during type 2 allergic response challenge and asthma exacerbation, with reproduction of hallmark features of severe asthma and epithelial damage. Indeed, administration of synthetic STING agonist diABZI during HDM challenge induces asthma exacerbation by increasing epithelial damage, dsDNA release, DNA damage, cell death by NETosis and PANoptosis, and neutrophils influx in the lung. We highlight the partial requirement for STING expression in granulocytes/macrophages to induce asthma exacerbation. We show that co-stimulation of human epithelial cells with diABZI and HDM induces IL-6, TNF-α, type I IFNα/β and type III IFNλ release *in vitro*, with DNA damage and cell death. These results have important implications revealing STING agonists as inducers of asthma exacerbation and offer a mechanism through which dsDNA release after cell death triggers Th1 response and promotes neutrophilic asthma exacerbation.

Host DNA released from dying cells was shown to mediate alum adjuvant activity [7], and cGAMP may function as a type 2 adjuvant promoting allergic asthma when administered during sensitization with HDM [10]. Our previous findings showing neutrophilic response induced by STING agonists in the airways [12] prompted us to ask whether triggering STING during HDM-challenge might affect the allergic response and promote a neutrophilic exacerbation.

The potent STING agonist diABZI administered during HDM-challenge strongly exacerbated neutrophil recruitment and the release of IFNγ, CXCL1/KC and CXCL10/IP10 in the airways. It induced some cell stress with extracellular dsDNA release, mobilized DNA sensors, and promoted an IFNα/β response. Importantly, administration of diABZI during HDM-challenge functionally exacerbated HDM-induced lung resistance, while Poly(I:C) did not affect lung function. We verified that diABZI-induced neutrophilic response in HDM-challenged mice is fully dependent on STING pathway, as it is absent in STING-deficient mice, and showed a

limited involvement of cGAS. The increased neutrophil recruitment, together with the presence of extracellular DNA, MPO and Cit-H3 was indicative of NETs formation, that were indeed visible in the airways of HDM challenged mice after cGAMP or diABZI administration. Thus, STING agonist induction of NETosis may contribute to the neutrophilic exacerbation of HDM-induced responses.

STING agonists led to a reduction of goblet cell numbers and of mucus transcript in the lung of HDM-challenged mice, together with a strong release of mucus protein in the airways. A possible explanation is that diABZI induced epithelial barrier damage, documented by epithelium cell tight junction ZO-1 protein expression, leading to Goblet cells shedding and release of their mucus content, that may clog the airspace and contribute to the exacerbation of HDM-induced lung resistance.

Several soluble mediators regulate the recruitment of neutrophils in the airways [24]. Indeed, diABZI induced IFNγ, CXCL1/KC and CXCL10/IP10 release *in vivo* in the BAL of HDM-challenged mice, and CXCL8 *in vitro* in the supernatant of human epithelial cells. These mediators are potent neutrophil chemoattractants in the lung, CXCL10 facilitating the recruitment of Th1 cells producing IFNγ which, in turn, upregulates chemotaxis receptors of human neutrophils [33]. Functional type I IFN signaling in neutrophils induces neutrophil maturation, and limits their lifespan by acting on both extrinsic and intrinsic apoptosis pathways but also by influencing the NETosis process [34]. Indeed, we show increased mature neutrophils expressing high CXCR2 or CXCR4 in the airways after diABZI during HDM-challenge.

Type I IFNs are essential regulators of neutrophil polarization, as shown in cancer, driving neutrophils from anti-inflammatory, pro-tumoral N2 phenotype into pro-inflammatory, anti-tumoral N1 capable of cytotoxicity [34,35]. Here, we demonstrate that STING agonists strongly induced N1 ($NOS2^{+}ARG1^{-}$) subset. This phenotypic shift from N2 ($ARG1^{+}NOS2^{-}$) observed at HDM baseline response toward N1 pro-inflammatory after STING agonist challenge, may

shape neutrophils function and enroll them in NETs formation process, in part responsible of lung tissue damage. Conversely, the N2 ($ARG1^+$ $NOS2^-$) profile of Poly(I:C)-induced neutrophils may explain the lack of NET in the lung of Poly(I:C) treated HDM challenged mice. NOS2 and ARG1 are important enzymes regulating both macrophage and neutrophil functions and markers of alternative activation [36,37]. NOS2 has multiple roles in the airways, its expression being highest in severe asthma, while ARG1 decreases [38-41]. We report increased NOS2 expression in RV-A16 infected patients with asthma, as compared to healthy controls. Further, transcriptomic analyses of RV-A16 infected cells from patients with asthma also indicated an involvement of DNA sensing, PANoptosis, and weakening of the epithelial barrier. Our study is the first to demonstrate the induction of this particular subset of N1, $NOS2^+ARG1^-$neutrophils following STING activation.

Triggering STING in an allergic context may shape the inflammatory response toward a mixed Th1/Th2 immune response and recapitulate features of severe neutrophilic asthma with increased lung resistance, NETosis and PANoptosis, increased epithelial injury, release of extracellular dsDNA and pro-inflammatory cytokines in the airways. Thus, targeting the STING pathway might be considered in severe asthma including seasonal respiratory viral exacerbation.

Author Contributions

Y.M.-N. performed most experiments with the assistance of E.C. and S.R. B.M. generated the STING-OST^{fl} mouse model. Y.M.-N., D.T., B.R. and V.Q. conceived the project and designed the experiments, Y.M.-N., D.T., B.R., V.Q., G.dS., M.E., D.J., S.J., M.S. and U.R. analyzed and interpreted the data. Y.M.-N, D.T., B.R. and V.Q. wrote the manuscript. All authors had the opportunity to discuss the results and comment on the manuscript.

Funding Statement

This work was supported by CNRS, University of Orleans, 'Fondation pour la Recherche Médicale' (FRM EQU202003010405), Region Centre-Val de Loire (ExAsPIR17 N° 2021-00144721), European funding in Region Centre-Val de Loire (FEDER EUROFeri N° EX010381 and TARGET-Ex N° EX016008), ANR-10-INSB-07 and CIPHE (supported by the "investissement d'avenir programme PHENOMIN" (French National infrastructure for mouse Phenogenomics). The human in vivo work was supported by the European Research Council (ERC FP7 Advanced grant number 233015); a Chair from Asthma UK (CH11SJ); the Medical Research Council Centre (grant number G1000758); National Institute of Health Research (NIHR) Biomedical Research Centre (grant number P26095); Predicta FP7 Collaborative Project (grant number 260895); and the NIHR Biomedical Research Centre at Imperial College London.

Total word count: text: 3426 words

This article has an online data supplement, which is accessible at Allergy online Repository Materials.

Conflict of interest statement

M.S. reports research grants from Swiss National Science Foundation (nr 310030_189334/1), Novartis Foundation for Medical-Biological Research, GSK, and Stiftung vorm. Buendner Heilstaette Arosa; speaker's fee from AstraZeneca; voluntary positions in the European Academy of Allergy and Clinical Immunology (EAACI) as Executive Board member and Basic and Clinical Immunology Section Chair. S.L.J. reports grants/contracts from European Research Council ERC FP7 grant number 233015, Chair from Asthma UK CH11SJ, Medical Research Council Centre grant number G1000758, NIHR Biomedical Research Centre grant number P26095, Predicta FP7 Collaborative Project grant number 260895, NIHR Emeritus NIHR Senior Investigator; consulting fees from Lallemand Pharma, Bioforce, resTORbio, Gerson Lehrman Group, Boehringer Ingelheim, Novartis, Bayer, Myelo Therapeutics GmbH; patents issued/licensed: Wark PA, Johnston SL, Holgate ST, Davies DE. Anti-virus therapy for respiratory diseases. UK patent application No. GB 0405634.7, 12March 2004. Wark PA, Johnston SL, Holgate ST, Davies DE. Interferon-Beta for Anti-Virus Therapy for Respiratory Diseases. International Patent Application No. PCT/GB05/50031, 12 March 2004. Davies DE, Wark PA, Holgate ST, Johnston SL. Interferon Lambda therapy for the treatment of respiratory disease. UK patent application No. 6779645.9, granted15th August 2012; Participation on a data safety monitory board or advisory board: Enanta Chair of DSMB, Virtus Respiratory Research Ltd Shareholder and Board membership. All other authors declare no competing interests

Ethics Statement

All animal experiments complied with the French Government animal experiment regulations and ARRIVE guidelines. The protocols were submitted to the "Ethics Committee for Animal

Experimentation of CNRS Campus Orleans" under the number CLE CCO 2019-2017 and 2020-2006, and approved by the French Government animal experiment regulatory authorities under APAFIS #25876 and #26195. In vivo rhinovirus infection in controls and patients with asthma was approved by the St. Mary`s Hospital Research Ethics Committee (United Kingdom), permission number 09/H0712/59 (observational trial registration number NCT01159782) [31,32].

Data Availability Statement

All datasets generated and analyzed during this study are included in this published article and its Supplementary Information files. Publicly available Transcriptome data from bronchial brushings from control individuals and patients with asthma infected in vivo with RV are available under accession number: GSE185658 [32]. Publicly available RNAseq data GSE61141 were downloaded from the NCBI gene expression omnibus [30,32]. Additional data are available from corresponding author on reasonable request. The PBMCs scRNAseq datasets from patients with severe asthma and control individuals analyzed in the present study, have been deposited in the Sequence Read Archive (SRA) repository under the accession number GSE172495 [42].

References:

1. Hammad H, Lambrecht BN. The basic immunology of asthma. *Cell.* 2021;184(6):1469-1485.
2. Schiffers C, Hristova M, Habibovic A, et al. The Transient Receptor Potential Channel Vanilloid 1 Is Critical in Innate Airway Epithelial Responses to Protease Allergens. *Am J Respir Cell Mol Biol.* 2020;63(2):198-208.
3. Agache I. Severe asthma phenotypes and endotypes. *Semin Immunol.* 2019;46:101301.
4. Cardoso-Vigueros C, von Blumenthal T, Ruckert B, et al. Leukocyte redistribution as immunological biomarker of corticosteroid resistance in severe asthma. *Clin Exp Allergy.* 2022;52(10):1183-1194.
5. Fahy JV. Type 2 inflammation in asthma--present in most, absent in many. *Nat Rev Immunol.* 2015;15(1):57-65.
6. Lambrecht BN, Hammad H, Fahy JV. The Cytokines of Asthma. *Immunity.* 2019;50(4):975-991.
7. Marichal T, Ohata K, Bedoret D, et al. DNA released from dying host cells mediates aluminum adjuvant activity. *Nat Med.* 2011;17(8):996-1002.
8. Decout A, Katz JD, Venkatraman S, Ablasser A. The cGAS-STING pathway as a therapeutic target in inflammatory diseases. *Nat Rev Immunol.* 2021;21(9):548-569.
9. Han Y, Chen L, Liu H, et al. Airway Epithelial cGAS Is Critical for Induction of Experimental Allergic Airway Inflammation. *J Immunol.* 2020;204(6):1437-1447.
10. Ozasa K, Temizoz B, Kusakabe T, et al. Cyclic GMP-AMP Triggers Asthma in an IL-33-Dependent Manner That Is Blocked by Amlexanox, a TBK1 Inhibitor. *Front Immunol.* 2019;10:2212.
11. Raundhal M, Morse C, Khare A, et al. High IFN-gamma and low SLPI mark severe asthma in mice and humans. *J Clin Invest.* 2015;125(8):3037-3050.

12. Messaoud-Nacer Y, Culerier E, Rose S, et al. STING agonist diABZI induces PANoptosis and DNA mediated acute respiratory distress syndrome (ARDS). *Cell Death Dis.* 2022;13(3):269.
13. Ahn J, Gutman D, Saijo S, Barber GN. STING manifests self DNA-dependent inflammatory disease. *Proc Natl Acad Sci U S A.* 2012;109(47):19386-19391.
14. Li XD, Wu J, Gao D, Wang H, Sun L, Chen ZJ. Pivotal roles of cGAS-cGAMP signaling in antiviral defense and immune adjuvant effects. *Science.* 2013;341(6152):1390-1394.
15. Ramanjulu JM, Pesiridis GS, Yang J, et al. Design of amidobenzimidazole STING receptor agonists with systemic activity. *Nature.* 2018;564(7736):439-443.
16. Chapman DG, Irvin CG. Mechanisms of airway hyper-responsiveness in asthma: the past, present and yet to come. *Clin Exp Allergy.* 2015;45(4):706-719.
17. Lemanske RF, Jr., Busse WW. Asthma: clinical expression and molecular mechanisms. *J Allergy Clin Immunol.* 2010;125(2 Suppl 2):S95-102.
18. Wang X, Li Y, Luo D, et al. Lyn regulates mucus secretion and MUC5AC via the STAT6 signaling pathway during allergic airway inflammation. *Sci Rep.* 2017;7:42675.
19. Porto BN, Stein RT. Neutrophil Extracellular Traps in Pulmonary Diseases: Too Much of a Good Thing? *Front Immunol.* 2016;7:311.
20. Vorobjeva NV, Pinegin BV. Neutrophil extracellular traps: mechanisms of formation and role in health and disease. *Biochemistry (Mosc).* 2014;79(12):1286-1296.
21. Radermecker C, Detrembleur N, Guiot J, et al. Neutrophil extracellular traps infiltrate the lung airway, interstitial, and vascular compartments in severe COVID-19. *J Exp Med.* 2020;217(12).

22. Chen L, Xu J, Deng M, et al. Telmisartan mitigates lipopolysaccharide (LPS)-induced production of mucin 5AC (MUC5AC) through increasing suppressor of cytokine signaling 1 (SOCS1). *Bioengineered.* 2021;12(1):3912-3923.
23. Zhang CX, Ye SB, Ni JJ, et al. STING signaling remodels the tumor microenvironment by antagonizing myeloid-derived suppressor cell expansion. *Cell Death Differ.* 2019;26(11):2314-2328.
24. Ray A, Kolls JK. Neutrophilic Inflammation in Asthma and Association with Disease Severity. *Trends Immunol.* 2017;38(12):942-954.
25. She L, Barrera GD, Yan L, et al. STING activation in alveolar macrophages and group 2 innate lymphoid cells suppresses IL-33-driven type 2 immunopathology. *JCI Insight.* 2021;6(3).
26. Akdis CA. Does the epithelial barrier hypothesis explain the increase in allergy, autoimmunity and other chronic conditions? *Nat Rev Immunol.* 2021;21(11):739-751.
27. Tan HT, Hagner S, Ruchti F, et al. Tight junction, mucin, and inflammasome-related molecules are differentially expressed in eosinophilic, mixed, and neutrophilic experimental asthma in mice. *Allergy.* 2019;74(2):294-307.
28. Xiao C, Puddicombe SM, Field S, et al. Defective epithelial barrier function in asthma. *J Allergy Clin Immunol.* 2011;128(3):549-556 e541-512.
29. Toussaint M, Jackson DJ, Swieboda D, et al. Host DNA released by NETosis promotes rhinovirus-induced type-2 allergic asthma exacerbation. *Nat Med.* 2017;23(6):681-691.
30. Bai J, Smock SL, Jackson GR, Jr., et al. Phenotypic responses of differentiated asthmatic human airway epithelial cultures to rhinovirus. *PLoS One.* 2015;10(2):e0118286.

31. Jackson DJ, Makrinioti H, Rana BM, et al. IL-33-dependent type 2 inflammation during rhinovirus-induced asthma exacerbations in vivo. *Am J Respir Crit Care Med.* 2014;190(12):1373-1382.

32. Radzikowska U, Eljaszewicz A, Tan G, et al. Rhinovirus-induced epithelial RIG-I inflammasome suppresses antiviral immunity and promotes inflammation in asthma and COVID-19. *Nat Commun.* 2023;14(1):2329.

33. Bonecchi R, Polentarutti N, Luini W, et al. Up-regulation of CCR1 and CCR3 and induction of chemotaxis to CC chemokines by IFN-gamma in human neutrophils. *J Immunol.* 1999;162(1):474-479.

34. Pylaeva E, Lang S, Jablonska J. The Essential Role of Type I Interferons in Differentiation and Activation of Tumor-Associated Neutrophils. *Front Immunol.* 2016;7:629.

35. Wang X, Qiu L, Li Z, Wang XY, Yi H. Understanding the Multifaceted Role of Neutrophils in Cancer and Autoimmune Diseases. *Front Immunol.* 2018;9:2456.

36. Garcia-Navas R, Gajate C, Mollinedo F. Neutrophils drive endoplasmic reticulum stress-mediated apoptosis in cancer cells through arginase-1 release. *Sci Rep.* 2021;11(1):12574.

37. Murray PJ. Macrophage Polarization. *Annu Rev Physiol.* 2017;79:541-566.

38. Cloots RHE, Poynter ME, Terwindt E, Lamers WH, Kohler SE. Hypoargininemia exacerbates airway hyperresponsiveness in a mouse model of asthma. *Respir Res.* 2018;19(1):98.

39. Litonjua AA, Lasky-Su J, Schneiter K, et al. ARG1 is a novel bronchodilator response gene: screening and replication in four asthma cohorts. *Am J Respir Crit Care Med.* 2008;178(7):688-694.

628 40. Maarsingh H, Dekkers BG, Zuidhof AB, et al. Increased arginase activity contributes to
629 airway remodelling in chronic allergic asthma. *Eur Respir J.* 2011;38(2):318-328.
630 41. Yamamoto M, Tochino Y, Chibana K, Trudeau JB, Holguin F, Wenzel SE. Nitric oxide
631 and related enzymes in asthma: relation to severity, enzyme function and inflammation.
632 *Clin Exp Allergy.* 2012;42(5):760-768.
633 42. Chen A, Diaz-Soto MP, Sanmamed MF, et al. Single-cell characterization of a model
634 of poly I:C-stimulated peripheral blood mononuclear cells in severe asthma. *Respir Res.*
635 2021;22(1):122.

636

637

Figures legends

Figure 1: Endogenous STING agonists promote lung neutrophilia and exacerbate allergic airway inflammation.

(A) Mice sensitized with HDM on day 0 and 7 (25 μg/mouse, i.n.) and challenged with HDM on day 14-16 (10 μg/mouse, i.n.) received either diABZI (1 μg/mouse, i.t.), cGAMP (10 μg/mouse, i.t.), or Poly(I:C) (200 μg/mouse, i.t.) on day 14-16, and were analyzed on day 17. **(B)** Airway resistance to increased doses of methacholine (50-200 mg/mL Mch) was measured 24h after the last HDM/agonist challenges. **(C)** Eosinophil and **(D)** neutrophil counts in BAL. **(E)** Flow cytometry analysis of NOS2/ARG1 expressing neutrophils pre-gated on singlet cells, and $CD45^+CD11b^+Ly6G^+F4/80^-SiglecF^-$ cells. **(F, G)** Myeloperoxidase (MPO) concentrations in BALF and lung determined by ELISA. **(H)** dsDNA measured in the acellular fraction of the BAL. **(I)** IFNγ, **(J)** IFN-α and **(K)** IFN-β concentrations in BALF measured by multiplex immunoassay. **(L)** Histology of lung sections stained with PAS, with semi quantitative pathology scoring of **(M)** goblet cells, **(N)** peribronchial infiltrates and **(O)** epithelial injury. Bars, left panel: 2.5 mm, right panel: 250 μm. **(P)** *Muc5ac* transcripts measured by real-time PCR **(Q, R)** Muc5ac protein in BALF and lung measured by ELISA. **(S)** Immunoblots of phospho-STAT6 and STAT6 with Actinβ as a reference. Data were presented as mean ± SEM with n = 8 mice per group. Each point represents an individual mouse. *$p < 0.05$, **$p < 0.01$, ***$p < 0.001$, ****$p < 0.0001$ (Nonparametric Kruskal–Wallis with Dunn's post-test).

Figure 2: NETosis, apoptosis, pyroptosis and necroptosis (PANoptosis) as main sources of airway dsDNA exacerbating HDM-induced lung inflammation.

Mice sensitized and challenged with HDM received either diABZI, cGAMP, or Poly(I:C) as in Figure 1, and were analyzed on day 17. **(A)** Visualization of NETs formation in lung tissue with the staining of DNA dye DAPI (Blue) and MPO (Yellow). Bars (20 μm). Tissue fluorescence

intensity (TFI) of MPO staining in lung. **(B)** Immunoblot highlighting DNA damage with expression of Cit-H3 phospho-γH2AX and γH2AX with Actinβ as a reference. **(C)** Immunoblot of STING axis including phospho-STING, STING dimer, STING, phospho-TBK1, TBK1 and DNA sensors including cGAS, DDX41 and IFI204 with Actinβ as a reference. **(D)** Immunoblot of inflammasome activation including AIM2, NLRP3, Caspase-11, cleaved caspase-11, IL-1β, cleaved IL-1β and IL-18 with Actinβ as a reference. **(E)** Immunoblot of cell death axis showing cleaved caspase-3, caspase-3, MLKL, cleaved GSDMD, GSDMD, ZBP1, caspase-8, and RIPK3 with Actinβ as a reference. **(F)** Confocal microscopy showing Caspase-8 (green), ASC (red), RIPK3 (far-red/turquoise blue) and DNA dye DAPI (cyan) in BAL cells showing the colocalization of PANoptosome components. Bars, 2µm.

Figure 3: STING dependence of the neutrophilic airway inflammation exacerbation.
(A) Wild-type (WT), STING$^{-/-}$ or cGAS$^{-/-}$ mice were sensitized with HDM on day 0 and 7 (25 µg/mouse, i.n.), challenged with HDM on day 14-16 (10 µg/mouse, i.n.) without or with diABZI (1 µg/mouse, i.t.), and analyzed on day 17. **(B)** Neutrophils count in BAL. **(C, D)** MPO concentration in BALF and lung determined by ELISA. **(E)** dsDNA concentration in the BAL acellular fraction. **(F)** Protein concentration in BALF. **(G)** IFN-γ in BALF determined by multiplex immunoassay. **(H, I)** TNF-α in BALF and lung determined by ELISA. **(J)** IL-16 and **(K)** CXC10/IP-10 concentration in BALF measured by ELISA. **(L)** Histology of lung tissues stained with PAS of WT, STING$^{-/-}$ and cGAS$^{-/-}$ mice, with semi quantitative pathology scoring of **(M)** peribronchial infiltrates, **(N)** goblet cells and **(O)** epithelial injury. Bars, upper panel: 2.5 mm, lower panel: 250 µm. **(P-W)** *Muc5ac, Tmem173, Mb21d1, Il-13 Serpin1, Clc1, Spdef* and *Socs1* transcripts measured by real-time qPCR. Data were presented as mean ± SEM with n = 6 ~ 8 mice per group. Each point represents an individual mouse. *p < 0.05, **p < 0.01, ***p < 0.001, ****p < 0.0001 (Nonparametric Kruskal–Wallis with Dunn's post-test).

Figure 4: STING-deficient macrophages and granulocytes mitigates asthma exacerbation *in vivo* in the lung.

(A) STING-OST^{fl}LysM$^{cre/+}$ or STING-OST^{fl}LysM$^{+/+}$ mice were sensitized with HDM on day 0 and 7 (25 µg/mouse, i.n.), challenged with HDM on day 14-16 (10 µg/mouse, i.n.) without or with cGAMP (10 µg/mouse, i.t.), and analyzed on day 17. **(B)** Eosinophils and **(C)** Neutrophils counts in BAL. **(D)** MPO concentration in BALF measured by ELISA. **(E)** dsDNA measured in the acellular fraction of the BAL. **(F)** Concentration of IFN-α and **(G)** IFN-β in BALF measured by luminex immunoassay. **(H)** IL-6 concentration **(I)** and TNF-α concentration in BALF measured by ELISA**. (J)** Lung tissue histology with PAS staining of STING-OST^{fl}LysM^{cre+} or STING-OST^{fl}LysM$^{+/+}$ mice with semi quantitative pathology scoring of **(K)** peribronchial infiltrates, epithelial injury and goblet cells. **(L)** Visualization of NET in BAL with the staining of DNA dye DAPI (blue), MPO (Green), CitH3 (Red). Bars, 20 µm. Data were presented as mean ± SEM with n = 8 ~ 13 mice per group. Each point represents an individual mouse. *p < 0.05, **p < 0.01, ***p < 0.001, ****p < 0.0001 (Nonparametric Kruskal–Wallis with Dunn's post-test).

Figure 5. **Epithelial cells contribute to the process of STING agonists-induced neutrophilic asthma exacerbation**.

(A) Immunofluorescence staining of Zonulin-1 (ZO-1) (RED) in lung tissue sections from mice treated by HDM and challenged or not with diABZI, cGAMP, or Poly(I:C) as in Figure 1, counterstained with DAPI (Blue). Upper panel: 20µm, lower panel: 5µm. Immunoblots of human airway epithelial cell **(**hAEC**)** stimulated with HDM at 100 µg/mL alone or in combination with diABZI (10 µM), cGAMP (14 µM) or Poly(I:C) (100 µg/mL) for 2 or 24h

showing **(B)** STING pathway activation including phospho-STING, STING, phospho-TBK1, TBK1, phospho-IRF3, IRF3, phospho-STAT6 and STAT6, with Actinβ as a reference. **(C)** DNA damage and cell death axis including phospho-γH2AX, γH2AX, phospho-MLKL, MLKL and Actinβ as a reference. **(D-M)** Cytokines concentration of (**D, I**) IL-8/CXCL8, (**E, J**) IFN-β, (**F, K**) IP-10/CXCL10, (**G, L**) IL-6 and (**H, M**) TNF-α in cell culture supernatant were measured by multiplex immunoassay at 2h **(D-H)** and 24h **(I-M)**. Data were presented as mean ± SEM with n = 3 independent wells from the same donor. **(N)** Human airway epithelium (MUCILAIR™) from a single healthy or donor with asthma were restimulated on the apical face, with HDM at 100 µg/mL alone or in combination with diABZI at 10 µM, cGAMP at 14 µM or Poly(I:C) at 100 µg/mL. At 6h post-stimulation, **(O)** Lactate dehydrogenase (LDH) concentration was determined in the supernatant. **(P-U)** Multiplex immunoassay of IFN-α **(P)**, IFN-β **(Q)**, IFN-λ **(R)**, IP-10/CXCL-10 **(S)**, IL-6 **(T)** and TNF-α **(U)** concentrations in the supernatant. **(V)** *MUC5AC* transcripts measured by real-time PCR. **(W)** Immunoblot from epithelial cell homogenates from healthy and patients with asthma showing the expression of phospho-γgH2AX with Actinβ as a reference. Data were presented as mean ± SEM with n = 3 independent wells from the same donor. *$p < 0.05$. (D-M) Nonparametric Kruskal–Wallis with Dunn's post-test.

Figure 6. Upregulation of DNA sensing and PANoptosis pathways upon rhinovirus infection in patients with asthma

(A) Human bronchial epithelial cells (HBECs) from patients with asthma (n = 6) and healthy controls (n=6), were infected with RV-A16 for 24h, and subjected to transcriptome analysis. (B-E) Heatmaps presented together with the corresponding log2 fold change (FC) expression changes (black bars) of (B) STING pathway-related genes, (C) Tight junction genes set, (D) PANoptosis-related genes, after in vitro RV-A16 infection in controls compared to HBEC from patients with asthma. Transcriptomic data were processed with the workflow available on https://github.com/uzh/ezRun.

(E) Experimental in vivo RV RV-A16 infection in patients with asthma (n=17) and healthy individuals (n=7): Transcriptomic analysis of bronchial brushings 14 days before and 4 days after in vivo infection. (F-G) Heatmaps presented together with the corresponding log2 fold change (FC) expression changes (black bars) of (F) Tight junction genes set, (G) PANoptosis-related genes, after in vivo RV-A16 infection in controls compared to patients with asthma. (H) Heatmaps of neutrophilic signature before (right panel) and after (left panel) infection in controls compared to patients with asthma. (I) Violin plots representing gene expressing of *NOS2* and *ARG1* in healthy individual and patients with asthma, before (lower set) and after (Upper set) infection. Data was analyzed with Bioconductor microarray analysis workflow [https://www.bioconductor.org/packages/release/workflows/vignettes/arrays/inst/doc/arrays.html].

All Heatmaps display normalized gene expression across the groups (row normalization). Asterisks demonstrate significantly changed genes with threshold $p<0.05$. p-value: *<0.05; **<0.005; ***<0.0005, ****<0.00005. Publicly available data under accession number: GSE185658 and GSE61141. Source data are provided as Source Data files.

Figure 1

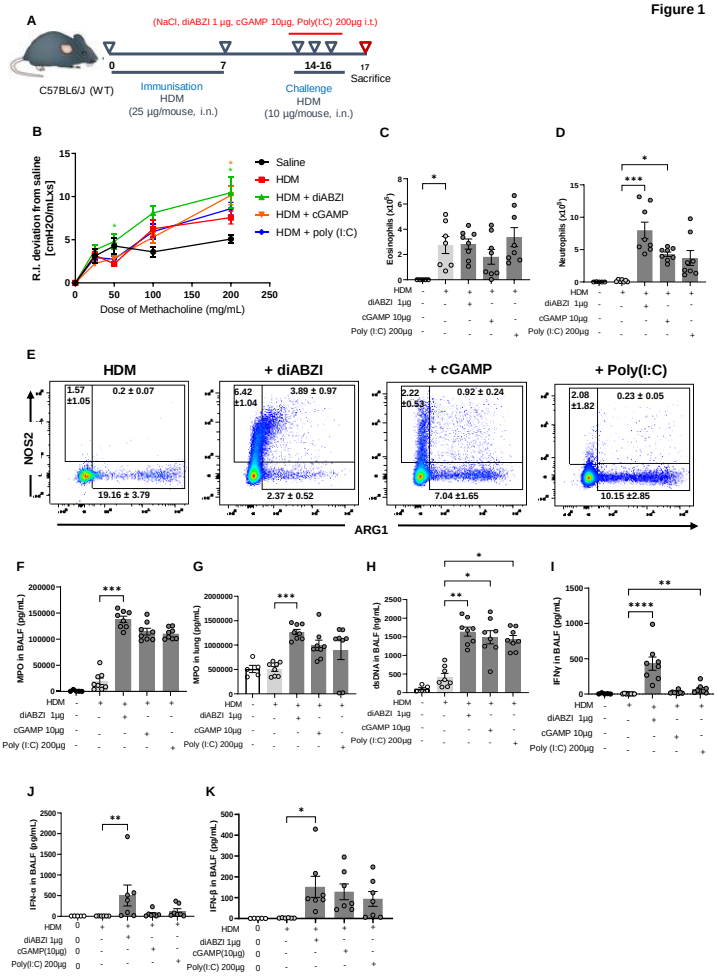
A
(NaCl, diABZI 1 µg, cGAMP 10µg, Poly(I:C) 200µg i.t.)
0
7
14-16
17
Sacrifice
C57BL6/J (WT)
Immunisation
HDM
(25 µg/mouse, i.n.)
Challenge
HDM
(10 µg/mouse, i.n.)
B
R.I. deviation from saline [cmH2O/mLXs]
Dose of Methacholine (mg/mL)
Saline
HDM
HDM + diABZI
HDM + cGAMP
HDM + poly (I:C)
C
Eosinophils (x10⁶)
D
Neutrophils (x10⁶)
HDM
diABZI 1µg
cGAMP 10µg
Poly (I:C) 200µg
E
HDM
+ diABZI
+ cGAMP
+ Poly(I:C)
NOS2
ARG1
1.57 ±1.05
0.2 ± 0.07
19.16 ± 3.79
6.42 ±1.04
3.89 ± 0.97
2.37 ± 0.52
2.22 ±0.53
0.92 ± 0.24
7.04 ±1.65
2.08 ±1.82
0.23 ± 0.05
10.15 ±2.85
F
MPO in BALF (pg/mL)
G
MPO in lung (pg/mL)
H
dsDNA in BALF (ng/mL)
I
IFNγ in BALF (pg/mL)
J
IFN-α in BALF (pg/mL)
K
IFN-β in BALF (pg/mL)

758

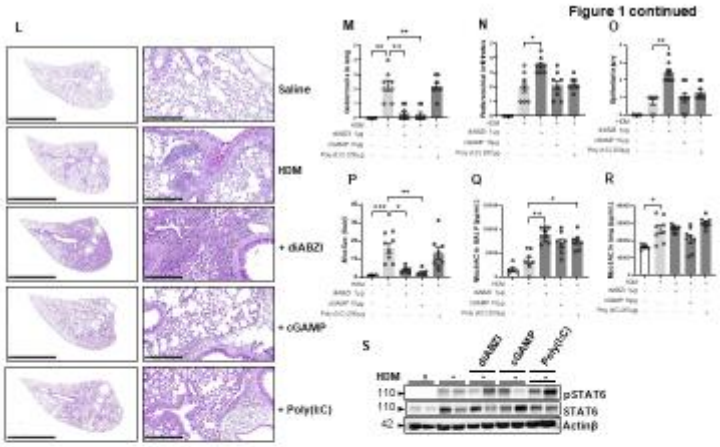
Figure 1 continued
L
M
N
O
P
Q
R
S
Saline
HDM
+ dABZI
+ cGAMP
+ Poly(I:C)
dABZI
cGAMP
Poly(I:C)
HDM
110
110
42
pSTAT6
STAT6
Actinβ

759

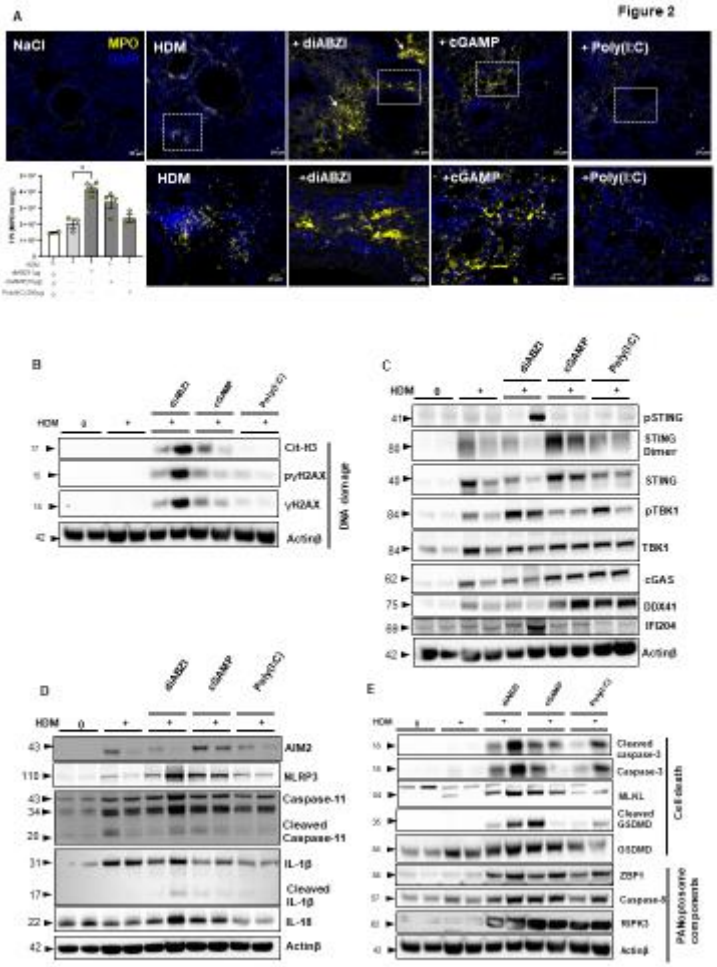
Figure 2
A
NaCl
MPO
HDM
+ diABZI
+ cGAMP
+ Poly(I:C)
B
C
D
E
Cit-H3
pγH2AX
γH2AX
Actinβ
DNA damage
pSTING
STING Dimer
STING
pTBK1
TBK1
cGAS
DDX41
IFI204
AIM2
NLRP3
Caspase-11
Cleaved Caspase-11
IL-1β
Cleaved IL-1β
IL-18
Cleaved caspase-1
Caspase-1
MLKL
Cleaved GSDMD
GSDMD
ZBP1
Caspase-8
RIPK3
Cell death
PANoptosome components

760

761

Figure 2 continued

F

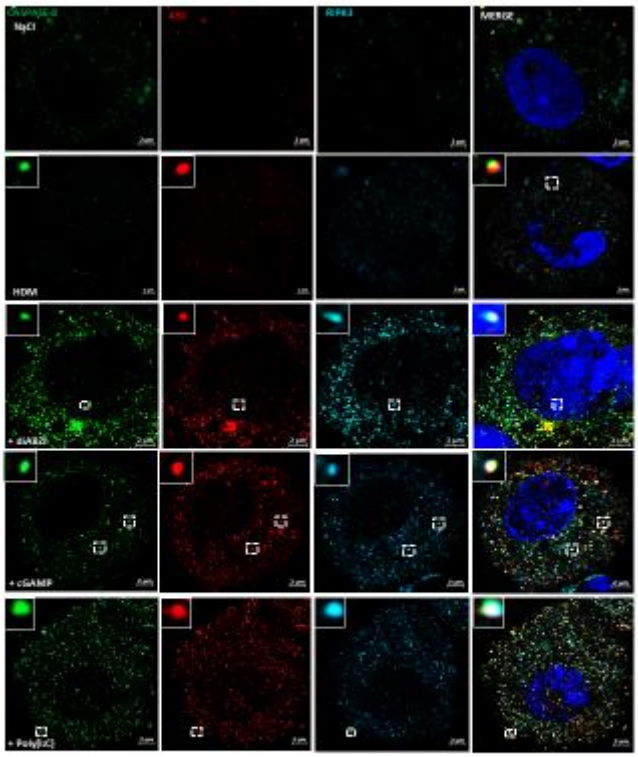

762

763

Figure 3

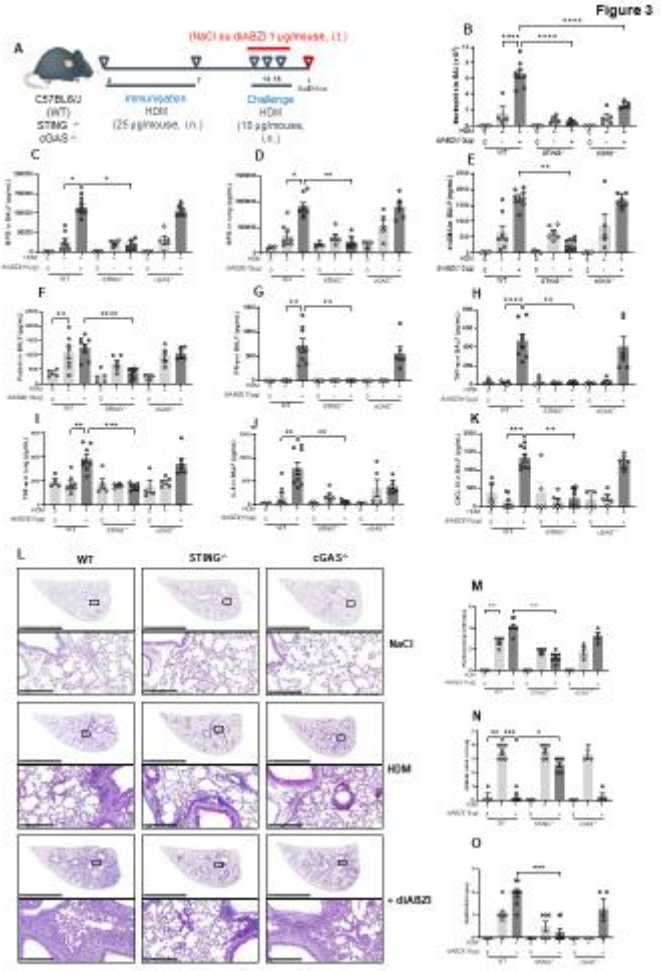

764

765

Figure 3 continued

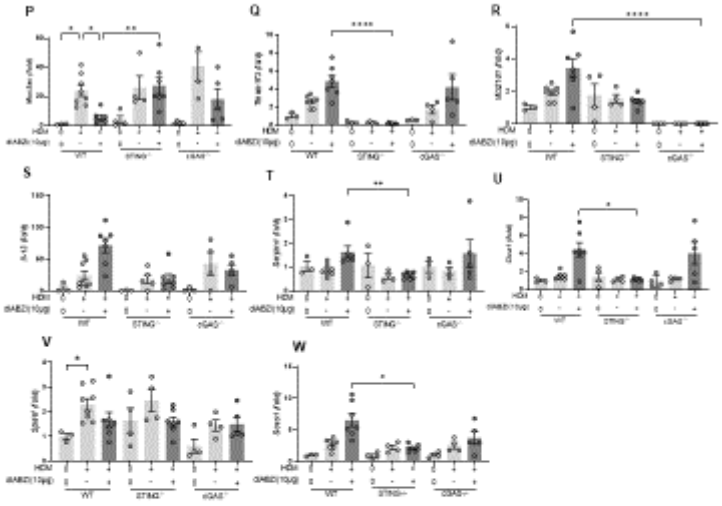

766

767

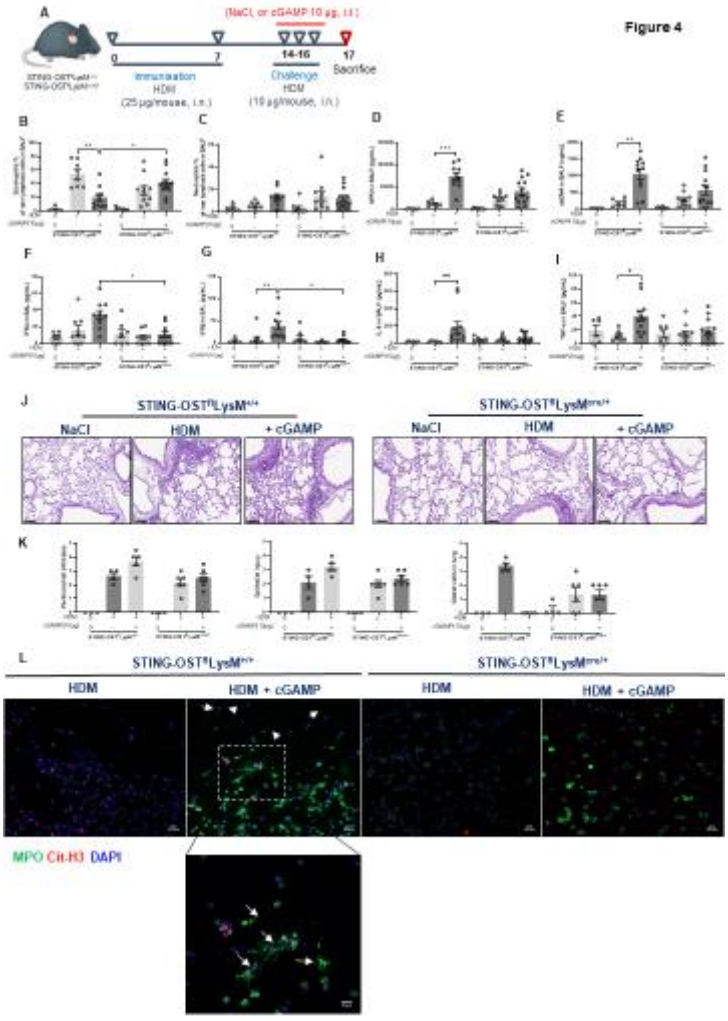

Figure 4

768

769

770

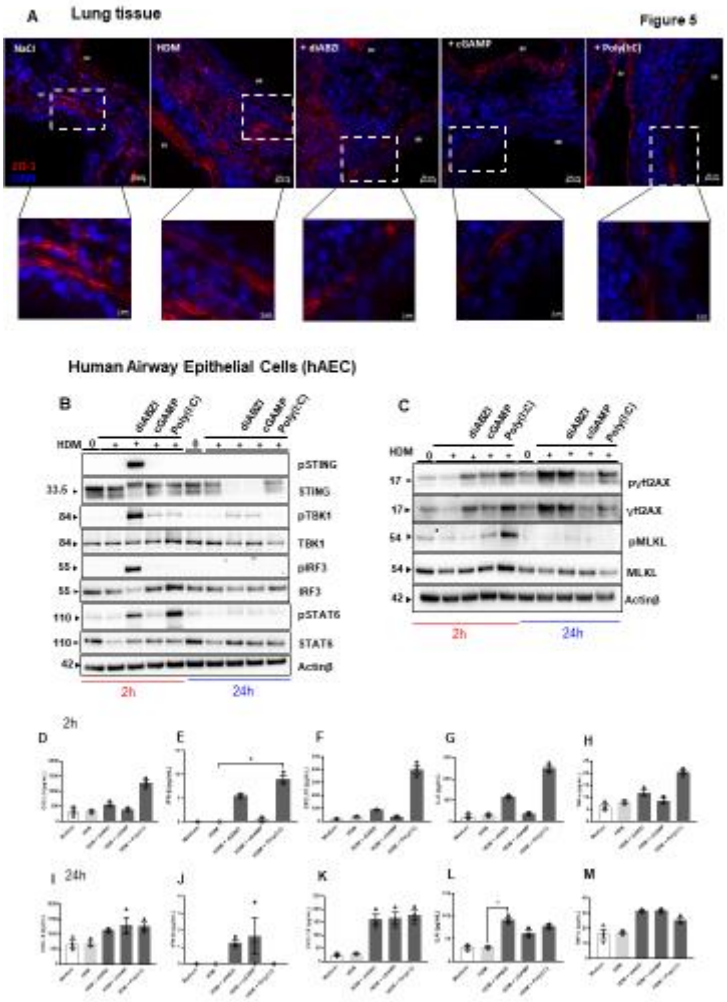
A
Lung tissue
Figure 5
NaCl
HDM
+ diABZI
+ cGAMP
+ Poly(I:C)
Human Airway Epithelial Cells (hAEC)
B
C
HDM
diABZI
cGAMP
Poly(I:C)
pSTING
STING
pTBK1
TBK1
pIRF3
IRF3
pSTAT6
STAT6
Actin
pγH2AX
γH2AX
pMLKL
MLKL
2h
24h
D
E
F
G
H
I
J
K
L
M

771

772

773

Figure 5 continued

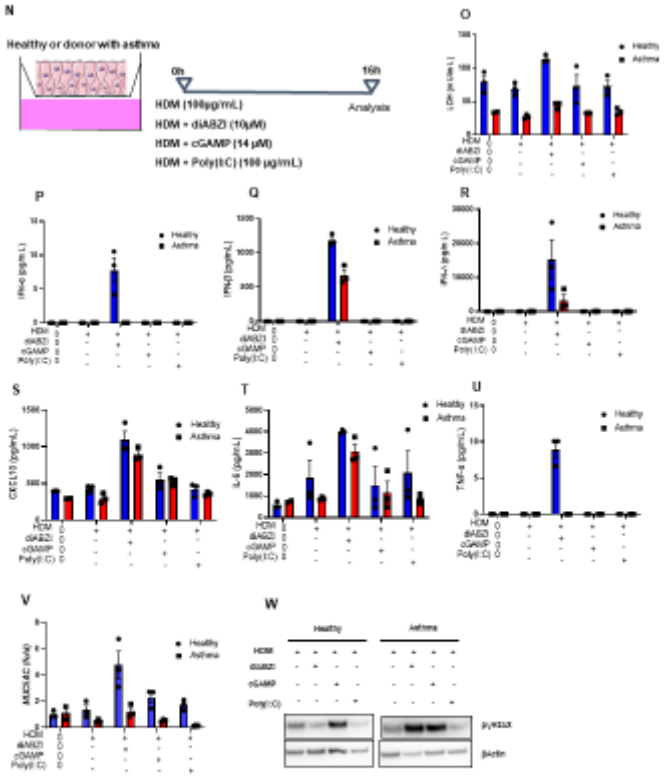

774

775

Figure 6

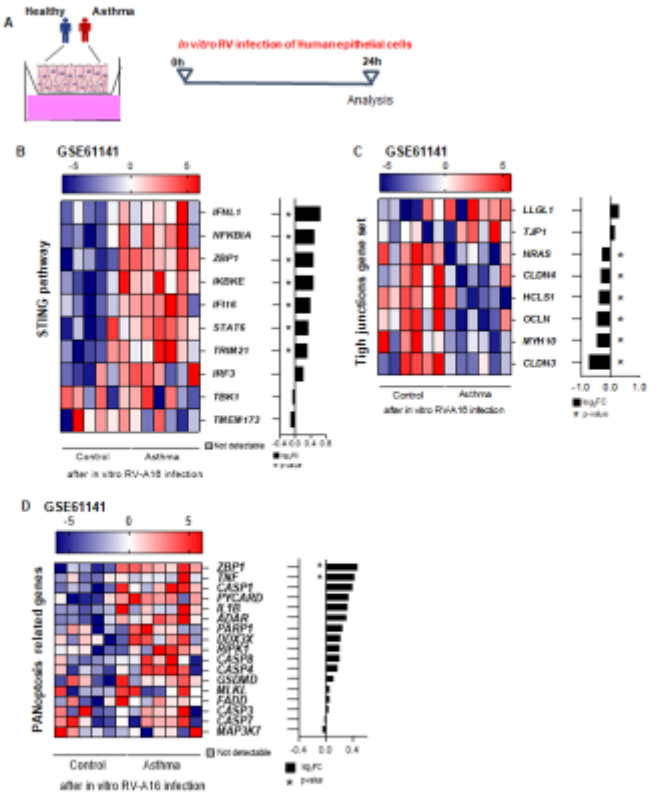

776

777

Figure 6 continued

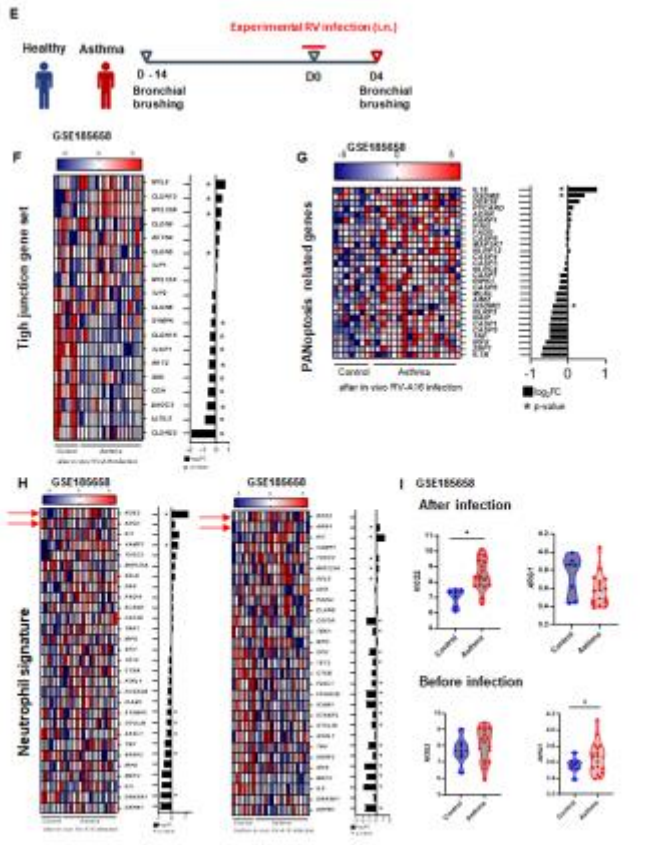

778

779

780